Raman-scattering and weak-ferromagnetism studies in Eu_2CuO_4

A. D. Alvarenga, D. Rao, J. A. Sanjurjo, E. Granado, I. Torriani, and C. Rettori
Instituto de Física "Gleb Wataghin," Universidade Estadual de Campinas, 13083-970 Campinas, São Paulo, Brazil

S. Oseroff
San Diego State University, San Diego, California 92182

J. Sarrao and Z. Fisk
Los Alamos National Laboratory, Los Alamos, New Mexico 87545
and National High Magnetic Field Laboratory, Florida State University, Tallahassee, Florida 32306

(Received 6 June 1995; revised manuscript received 19 September 1995)

We show that there is a subtle instability of the T' structure for the R_2CuO_4 (R=rare earth) compounds at the center of the R series with the boundary at Eu_2CuO_4. Crystals grown in Pt crucibles and PbO flux show weak ferromagnetism (WF) and two strongly temperature-dependent forbidden Raman peaks. However crystals grown in alumina crucibles and CuO flux do not show WF and the forbidden Raman peaks are much less intense. The observation of WF and forbidden Raman peaks for Eu_2CuO_4 compounds suggests that the instability of the T' structure may be associated with O(1) displacement in the CuO_2 planes.

I. INTRODUCTION

The $R_{2-x}M_xCuO_4$ compounds of T'-type structure (R=rare earths and M= Ce, Th) have been intensively studied since their discovery. For R= Pr, Nd, Sm, Eu, and $x \cong 0.15$, n-type superconductivity is achieved after appropriate thermal treatments in reducing atmospheres.[1] However the compounds with smaller rare-earth ionic radius (from Gd to Tm) are not superconductors for any doping concentration.[2] In all the undoped R_2CuO_4 compounds the copper moments order antiferromagnetically (AF) below $T_N \cong$ 240–280 K.[3] For heavier rare earths these compounds show weak ferromagnetism (WF), with a boundary at Eu_2CuO_4.[4] For R = Tb, Dy, Ho, Er, Tm, and Y, the T' structure can be synthesized only under high pressure, determining again a boundary for structural stability at the center of the rare-earth series.[5] The WF is associated with the canting in the **ab** plane of the Cu moments away from perfect AF alignment. In the T' ($I4/mmm$) structure WF order is forbidden, and lattice distortions in the CuO_2 planes must be invoked to account for WF. The existence of lattice distortions in Gd_2CuO_4 and Tm_2CuO_4 was invoked to explain the x-ray and Mössbauer data.[6] It was suggested that an in-plane lateral displacement of the O(1) atoms away from their symmetric positions in the CuO_2 planes may be responsible for a nonvanishing antisymmetric Dzyaloshinsky-Moriya exchange interaction between the Cu moments.[7,8] This distortion may be also responsible for the extra lines observed in Raman experiments of $Nd_{2-x}Gd_xCuO_4$ (Ref. 9) and Gd_2CuO_4.[10,11]

In this paper we present results of Raman and magnetization measurements in single crystals of Eu_2CuO_4, $Eu_{1.95}Ce_{0.05}CuO_4$, and $Eu_{2-x}Pr_xCuO_4$ (x=0.1, 0.25, and 1.0). For samples grown in Pt crucibles from PbO flux (hereafter, Pt/PbO), anomalous Raman peaks and WF are clearly observed. However for samples grown in alumina crucibles from CuO flux (hereafter, Al_2O_3/CuO), the intensity of the anomalous Raman peaks is strongly reduced and WF is not observed. These results suggest that for R= Eu, or smaller rare-earth ions the T' structure is subject to distortions in the CuO_2 planes, probably associated with O(1) displacements. That departure from a perfect tetragonal structure may be responsible for both the anomalous Raman peaks and WF.

II. EXPERIMENTAL DETAILS

The single crystals used in this work are of platelike shape with the **c** axis perpendicular to the large face. The crystals were grown from a nominally stoichiometric mixture of the respective oxides, using PbO and CuO fluxes in Pt and alumina crucibles, respectively. The Pb content was less than 1% of the copper content.[12] We should mention that it was not possible to grow Eu_2CuO_4 crystals in Al_2O_3 crucibles from PbO flux because the PbO flux aggressively attacked the Al_2O_3 crucible. For the Raman measurements the samples were mounted on the cold finger of a closed-cycle Displex He refrigerator. Two calibrated thermocouples, one near the samples and the other closer to the heater, allowed good temperature control from 10 to 300 K. The spectra were excited with the 514.5 nm line of an argon laser. A Jobin Yvon T6400 triple spectrometer with a charge coupled device camera was used to recorder the spectra. A backscattering geometry was used throughout. The magnetic measurements were made with a Quantum Design superconducting quantum interference device magnetometer. X-ray powder-diffraction measurements were performed using a Rigaku R200 diffractometer and rotating anode generator with Cu $K\alpha$ radiation. The lattice constants were calculated from the experimental data using a Rietveld profile refinement program.[13] A tetragonal unit cell with atomic positions of the T' structure ($SGI4/mmm$) was used for the calculations. The results are shown in Table I.

TABLE I. Lattice parameters (Å) of $Eu_{2-x}Pr_xCuO_4$ grown in Al_2O_3/CuO and Pt/PbO (see text). Values in parentheses are the standard deviations obtained from the Rietveld refinement analysis.

	$Eu_{2-x}Pr_xCuO_4$				
	Al_2O_3/CuO	Pt/PbO			
x	0.0	0.0	0.1	0.25	1.0
a	3.9021(2)	3.9084(2)	3.9081(4)	3.9112(10)	3.9247(3)
c	11.8948(5)	11.9093(2)	11.9422(16)	11.9404(8)	12.0522(8)

III. RAMAN RESULTS

A group-theoretical analysis predicts four Raman-active modes in the tetragonal T' structure: $A_{1g}+B_{1g}+2E_g$. Denoting by z the direction parallel to the crystal **c** axis, the modes appear at the configurations: $Y(ZZ)Y(A_{1g})$, $Y(ZX)Y$ (E_g), and $Z(XX)Z$ (B_{1g}). Figure 1 shows the 12 K Raman spectra for two samples of Eu_2CuO_4 prepared in Pt/PbO and Al_2O_3/CuO. For the Pt/PbO sample we identify Raman-active modes at 229 cm^{-1} (A_{1g}, z vibration of Eu atoms), 499 cm^{-1} [E_g, in plane out-of-phase vibrations of O(2) atoms] and 324 cm^{-1} [B_{1g}, out-of-plane vibrations of O(2) atoms].[14,15] As in Nd_2CuO_4 (Ref. 16) and Pr_2CuO_4,[17] the low energy E_g mode [in-plane vibrations of O(2) and Eu atoms] is not observed. The peaks at 413 cm^{-1} for XX polarization and 398 cm^{-1} for XY polarization do not correspond to any mode allowed in the T' structure. In Fig. 1 both peaks are, respectively, labeled B_{1g}^* and B_{2g}^* due to their polarization selection rules and allowed Raman tensor components of the irreducible representations for D_{4h} point symmetry. We will show below that they can be attributed to local modes associated with O(1) displacements

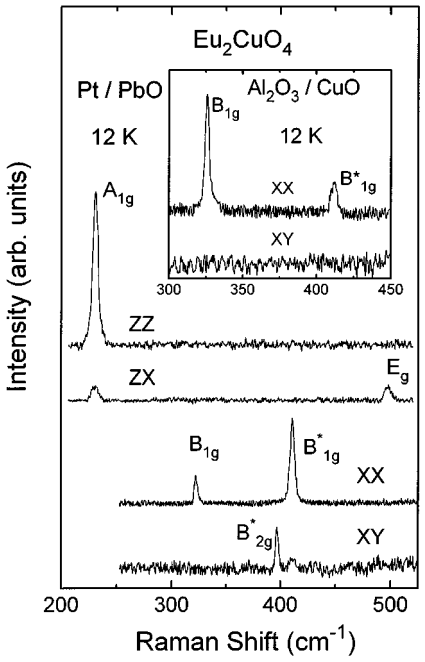

FIG. 1. Low-temperature Raman spectra of Eu_2CuO_4 grown in Pt/PbO and Al_2O_3/CuO for different polarizations. A_{1g}, B_{1g}, and E_g are the active Raman modes for the T' structure. B_{1g}^* and B_{2g}^* are the anomalous Raman peaks (see text).

in the CuO_2 planes.[7,8] Similar anomalous peaks have already been observed in Gd_2CuO_4. Laguna *et al.*[10] reported a symmetry-forbidden B_{1g} (XX) mode at 422 cm^{-1} and Udagawa *et al.*[11] another symmetry-forbidden B_{2g} (XY) mode at 380 cm^{-1}. Both authors, based on results of neutron and x-ray experiments[6,18] attributed these extra modes to local distortions in the CuO_2 planes and associated them to in-plane displacements of the O(1) atoms perpendicular to the Cu-O bonds. The symmetry and energy positions for the two additional peaks B_{2g}^* and B_{1g}^* in Eu_2CuO_4 suggest that their origin is the same as those found in Gd_2CuO_4. Based on the following considerations we conclude that the origin of the extra modes are related to local distortions associated with O(1) displacements in the CuO_2 planes: (1) Modes with higher energy than 300 cm^{-1} are only related to oxygen vibrations;[14] (2) The large energy separation ($\sim$ 95 cm^{-1}) between the anomalous peaks and the 499 cm^{-1} E_g mode indicate that those peaks cannot be associated to a splitting of the E_g mode. Splitting of the E_g mode is expected if the O(2) atoms would participate in the local distortions; (3) The distortions do not have long-range order, because the appearance of a superstructure should activate several new Raman modes, which are not observed in our experiments. Moreover in a recent work[19] on electron-spin resonance of Gd^{3+}(0.25%) in Eu_2CuO_4 grown in Al_2O_3/CuO no evidence was found for the presence of crystal distortions, although the Raman experiments still show the presence of the B_{1g}^* peak in this sample. This further confirms that the distortions do not have long-range order; (4) Displacements of the O(1) atoms perpendicular to the Cu-O bonds, suggested in Refs. 6 and 8, lower the local symmetry of the CuO_2 planes from tetragonal to orthorhombic and will activate two oxygen local modes, in agreement with the Raman results.

Figure 1 shows that in Eu_2CuO_4, the intensity of these anomalous peaks depends on how the samples were grown (i.e., Pt/PbO or Al_2O_3/CuO). The intensity of the B_{1g}^* peaks, relative to the B_{1g} mode, is greater for samples grown in Pt/PbO than for those grown in Al_2O_3/CuO. The B_{2g}^* peak is not observed in the Al_2O_3/CuO samples (see inset of Fig. 1).

Figures 2(a) and 2(b) show the Raman spectra of single crystals of $Eu_{2-x}Pr_xCuO_4$ ($x=0.0$, 0.1, 0.25, and 1.0) grown in Pt/PbO, for XX and XY polarizations, respectively. We see that the intensity of the anomalous peaks decreases with increasing Pr concentration. This behavior is expected in view of the stabilization of the T' structure toward the left side of the lanthanide series.[5]

In Fig. 3 we compare the Raman spectra of pure and 2.5% Ce-doped Eu_2CuO_4 single crystals grown in Pt/PbO. The introduction of Ce broadens the B_{1g} mode and the B_{1g}^* peak, but strongly decreases the intensity of the latter. Note that the B_{2g}^* peak is suppressed with a small doping of Ce. Thus Ce and Pr doping contribute to the stability of the structure and diminish the intensity of the anomalous Raman peaks.

The most striking result is the temperature dependence of the intensity of the anomalous peaks for samples grown by the two methods (Pt/PbO or Al_2O_3/CuO). Figures 4(a) and 4(b) show, respectively, the Raman spectra for XX and XY polarizations at different temperatures, for Pt/PbO samples. Lorentzian fits are used to obtain the Raman shift, linewidth, and intensity of the various peaks. The intensity of the B_{1g}

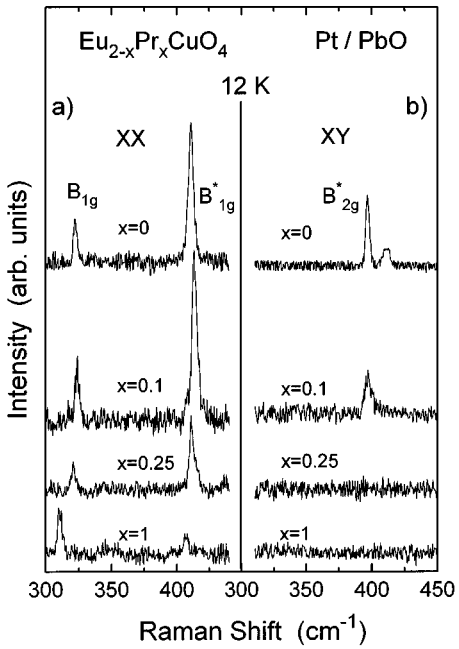

FIG. 2. Low-temperature Raman spectra of $Eu_{2-x}Pr_xCuO_4$ ($x=0.0$, 0.1, 0.25, and 1.0) grown in Pt/PbO for XX and XY polarizations.

mode was temperature independent. We used this to normalize the intensity of the B_{1g}^* peak. In Fig. 5 we plot the temperature dependence of the relative intensity between the B_{1g}^* peak and the B_{1g} mode. The temperature dependence of the intensity of the B_{2g}^* peak and the B_{1g} mode are also shown. We performed another set of measurements in which the three peaks were observed simultaneously. This is possible by rotating the incoming polarization about 22° away from the x axis, without using an analyzer. We found that the relative intensity between the B_{2g}^* peak and the B_{1g}^* peak is

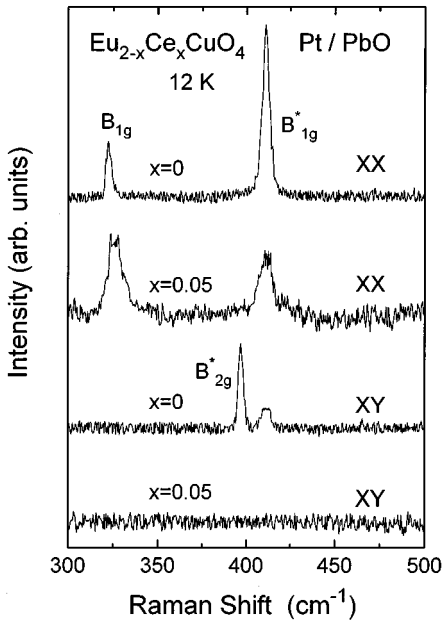

FIG. 3. Low-temperature Raman spectra of $Eu_{2-x}Ce_xCuO_4$ ($x=0.0$ and 0.05) grown in Pt/PbO for XX and XY polarizations.

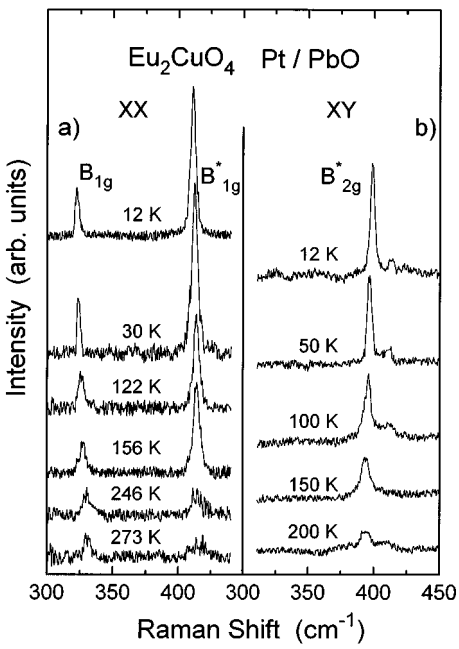

FIG. 4. Temperature dependence of the anomalous B_{1g}^* and B_{2g}^* Raman peaks in Eu_2CuO_4 grown in Pt/PbO.

almost temperature independent, indicating that both anomalous peaks have similar temperature dependence. It should be mentioned that in Gd_2CuO_4 the intensity of the B_{1g}^* peak is temperature independent.[10] Therefore in this compound the distortions are not temperature dependent, in agreement with x-ray results.[6]

IV. MAGNETIZATION RESULTS

Figure 6 shows the magnetization measured in the **ab** plane at 100 K after field cooling (FC) and zero-field cooling

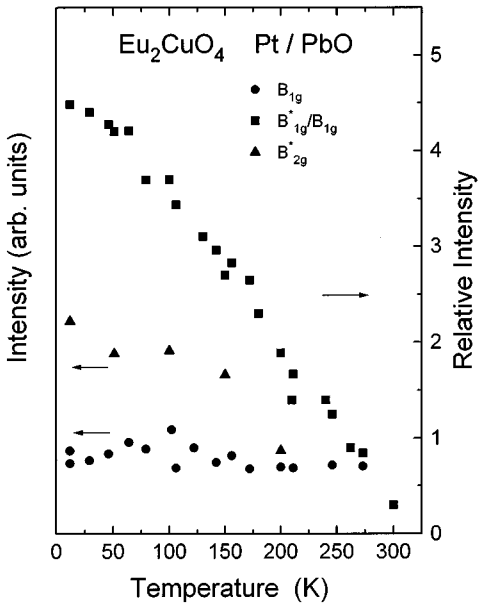

FIG. 5. Temperature dependence of the Raman intensity of the B_{1g} mode (full circles); the relative Raman intensity between the anomalous B_{1g}^* peak and the B_{1g} mode (full squares); and the Raman intensity of the anomalous B_{2g}^* peak (full triangles).

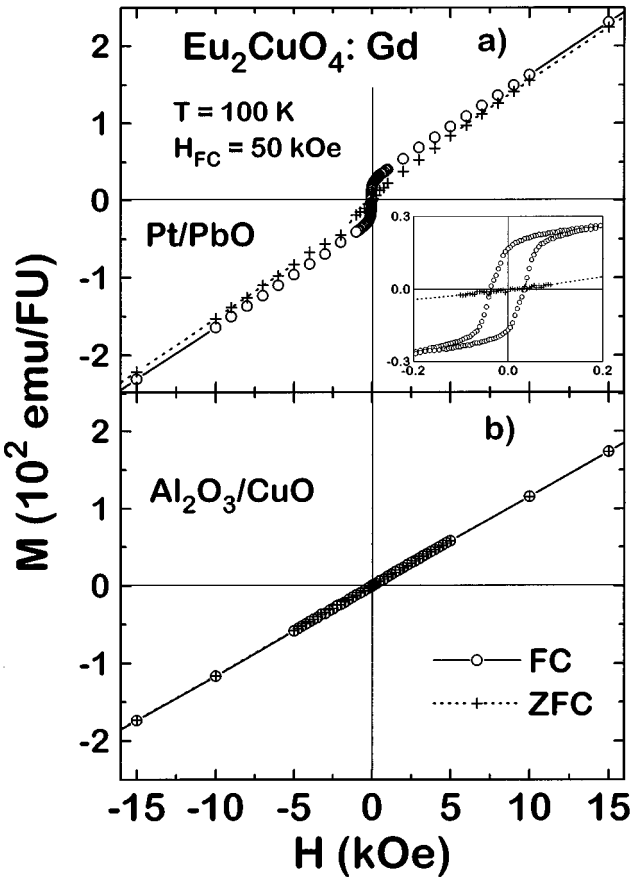

FIG. 6. Eu_2CuO_4:Gd **ab**-plane magnetization at $T=100$ K for ZFC and **ab** plane FC for (a) crystals grown in Pt/PbO and (b) crystals grown in Al_2O_3/CuO. The inset shows the FC hysteresis with $M_r \simeq 18(3)$ emu/f.u. and $H_c \simeq 40$ Oe.

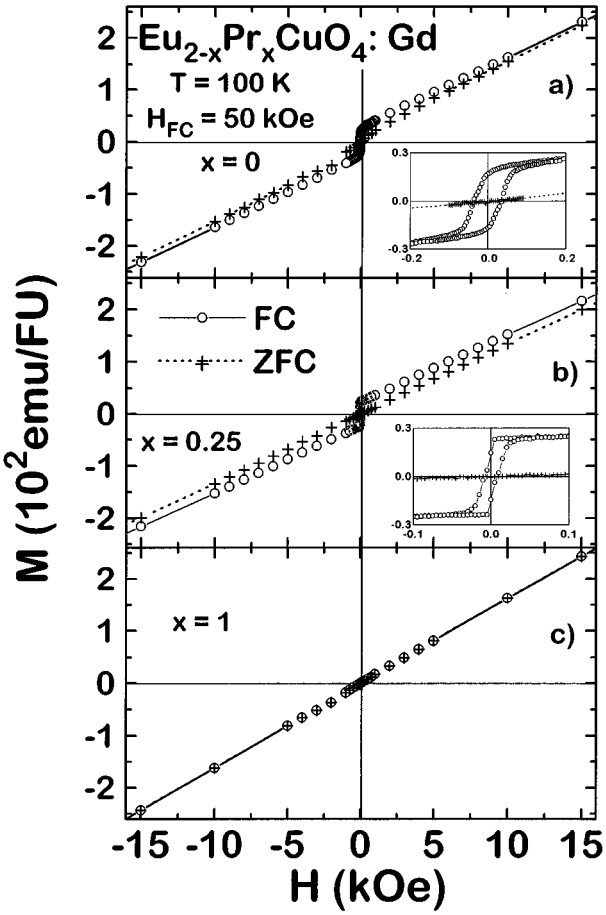

FIG. 7. $Eu_{2-x}Pr_xCuO_4$:Gd ($x=0.0$, 0.25, and 1.0) **ab**-plane magnetization at $T=100$ K for ZFC and **ab**-plane FC crystals grown in Pt/PbO. The inset of (a) shows the same hysteresis as Fig. 6(a) and the inset of (b) the hysteresis for $x=0.25$, with $M_r \simeq 15(3)$ emu/f.u. and $H_c \simeq 10$ Oe.

(ZFC), for the samples studied in Fig. 1. Figure 6(a) shows that for the sample grown in Pt/PbO, hysteresis and WF are observed after FC. The remnant magnetization (M_r) and the coercive magnetic field (H_c) depend on temperature and cooling field. The saturation values, $M_r^s \cong 22(5)$ emu/f.u. and $H_c^s \cong 50$–70 Oe, were measured at $T=20$ K when FC in 50 kOe. On the other hand, the ZFC magnetization is reversible and at $T \simeq 100$ K reaches the FC magnetization for fields higher than 10–15 kOe [see Fig. 6(a)]. For our applied fields, the anisotropy within the **ab** plane was negligible and no hysteresis or WF were detected perpendicular to the **ab** plane. Though Raman measurements still show the presence of the B_{1g}^* peak, we found no hysteresis or WF in samples grown in Al_2O_3/CuO [see Fig. 6(b)].

Figure 7 shows that for the samples studied in Fig. 2, the hysteresis and WF disappear as the Pr concentration increases. A similar behavior was found for the anomalous B_{1g}^* and B_{2g}^* Raman peaks (see Fig. 2). Moreover, we note that the sample doped with only 2.5% of Ce, (Fig. 3), showed no WF. These results strongly suggest that the anomalous B_{1g}^* and B_{2g}^* Raman peaks are associated with the presence of WF in these compounds.

Figure 8(a) shows the temperature dependence of the **ab**-plane magnetization for the samples of Fig. 1, measured at $H_{\text{app}} = 10$ kOe after FC in 50 kOe. While the samples grown in Pt/PbO show large difference between FC and ZFC [see Fig. 6(a)], the results for the samples grown in Al_2O_3/CuO showed no difference between FC and ZFC [see Fig. 6(b)]. Figure 8(b) shows the data of Fig. 8(a) after subtracting the contribution from Gd^{3+} impurities. Estimated Gd^{3+} concentrations were 0.55 and 0.25% for the samples grown in Pt/PbO and Al_2O_3/CuO, respectively. Figure 8(c) shows the difference in magnetization between the samples of Fig. 8(b). The magnetization measured perpendicular to the **ab** plane was found to be within 2%, the same for both samples. Therefore we can assume that the contribution of Eu^{3+} to the total **ab**-plane magnetization will be also the same in both samples. Thus the magnetization shown in Fig. 8(c) may be attributed to the canting of the Cu ions from perfect antiferromagnetic alignment, i.e., WF. This interpretation is further supported by the results shown in Fig. 6(a), where the ZFC magnetization reaches the FC magnetization at high field. Moreover Fig. 8(c) shows that the data can be approximately fitted to

$$M = M_0(1 - T/T_N)^{\beta}, \tag{1}$$

with $T_N = 241(5)$ K, $\beta = 0.51(2)$, and $M_0 = 39(2)$ emu/f.u. [corresponding to $6.8(3) \times 10^{-3}$ μ_B/Cu at $T \cong 10$ K]. This

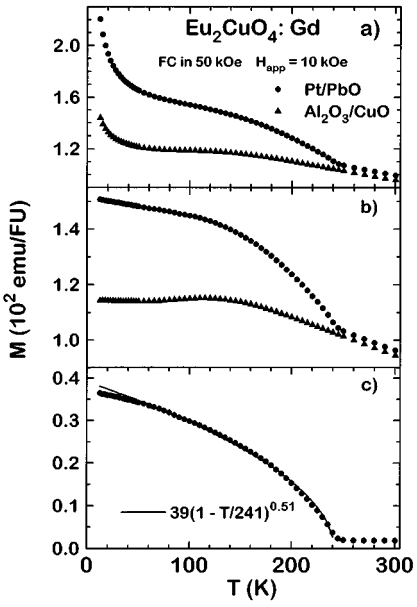

FIG. 8. Temperature dependence of the **ab**-plane magnetization for Eu_2CuO_4:Gd crystals grown in Pt/PbO and Al_2O_3/CuO measured in $H_{app} = 10$ kOe and after a FC of 50 kOe in the **ab** plane: (a) experimental data; (b) same as (a) after subtracting the contribution of 0.55% and 0.25% of Gd^{3+} for the crystals grown in Pt/PbO and Al_2O_3/CuO, respectively; and (c) difference between the data of (b).

value for the WF component of the Cu moment is in agreement with previous estimates.[20] The exponent $\beta = 0.51(2)$ suggests that a mean-field theory is a good approximation for the **ab** plane Cu magnetization. Since WF ordering of the Cu moments is forbidden in the T'-type structure, we claim that distortions in the CuO_2 planes of Eu_2CuO_4 are responsible for a nonvanishing antisymmetric Dzyaloshinsky-Moriya exchange interaction between the Cu moments.[8] Our Raman results suggest that these distortions are associated with O(1) displacements.

V. DISCUSSION

Table I shows the lattice parameters for most of the samples studied in this work. For the pure compound grown in Pt/PbO the lattice parameters are slightly larger than those of the compounds grown in Al_2O_3/CuO. Contamination with Pt from the crucible and/or Pb from the flux may be responsible for the difference in lattice parameters. At the end of this work we were able to grow Eu_2CuO_4 crystals in Pt crucible using CuO flux. The Raman results showed that the intensities of the B_{1g}^* and B_{2g}^* anomalous peaks lie between those found for samples grown in Pt/PbO and Al_2O_3/CuO. The FC magnetization measurements at $T = 100$ K showed WF with a smaller hysteresis loop $[M_r \cong 5(2)$ emu/f.u., $H_c \cong 7(3)$ Oe$]$ than that obtained for crystals grown in Pt/PbO. Therefore we conclude that both Pt and Pb impurities contribute to the distortions which give rise to the anomalous Raman peaks and WF in these compounds.

The anomalous Raman B_{1g}^* peak (see Fig. 5) is still observed above the Néel temperature ($T_N = 241$ K, determined by the appearance of WF). Therefore the distortions responsible for the B_{1g}^* and B_{2g}^* peaks may be associated with short-range magnetic ordering, and below T_N spin-dependent phonon Raman scattering[21] could be responsible for the increase of the intensity at low-temperatures. Alternatively, low-temperature lattice contractions may result in a larger number of these distortions, increasing the intensity of these Raman peaks at low temperatures.

From the Raman and WF results given above, the lattice parameters of Table I, and other works,[22–27] it is clear that a subtle instability in the T' structure occurs at a value of about **a** = 3.905(5) Å for the **ab**-plane lattice parameter. Compounds with smaller lattice parameters than this show WF, while those with larger lattice parameters may become superconductors when properly doped with Ce.[22]

VI. CONCLUSIONS

The experimental results presented above suggest that the anomalous Raman peaks in Eu_2CuO_4 are related to the appearance of WF. The addition of Pr or Ce increases the lattice volume and stabilizes the T' structure, leading to the disappearance of the anomalous Raman peaks and WF. The fact that all the compounds showing WF also show the anomalous peaks at about the same energy for all the R_2CuO_4 compounds, independent of dopant, crucible and used flux, supports the conclusion that these peaks are associated with local vibrations due to O(1) displacement. Contamination with Pt from the crucible and Pb from the flux may result in a larger number of displaced O(1) atoms in samples grown in Pt/PbO than for those grown in Al_2O_3/CuO. However lattice-dynamics calculations are needed in order to see how the anomalous Raman peaks can actually be associated with O(1) displacement in the CuO_2 planes. Also various experiments such as neutron diffraction, x-ray diffraction, Raman in FC samples and under pressure may give valuable information about the nature of the distortion and its temperature dependence.

ACKNOWLEDGMENTS

This work was supported by CNPq, Grant No. 91/0573-0 of FAPESP-São-Paulo-Brazil and No. NSF-DMR-9117212. A.D.A. and D.R. acknowledge financial support from CNPq. Work at Los Alamos was performed under the auspices of the United State Department of Energy. The NHMFL is supported by NSF Cooperative Agreement No. DMR-9016241.

[1] T. Markert and M.B. Maple, Solid State Commun. **70**, 145 (1989).
[2] H. Okada, M. Takano, and Y. Takeda, Physica C **166**, 111 (1990).
[3] R. Saez-Puche, M. Norton, and W.S. Glausinger, Mater. Res. Bull. **17**, 1523 (1982).
[4] S. Oseroff, D. Rao, F. Wright, M. Tovar, D.C. Vier, S. Schultz, J.D. Thompson, Z. Fisk, and S.W. Cheong, Phys. Rev. B **41**, 1934 (1990).
[5] P. Bordet, J.J. Capponi, C. Chaillaut, D. Chateigner, J. Chenavas, T. Fournier, J.L. Hodeau, M. Marezio, M. Perroux, G. Thomas,

and A. Varela, Physica C **185-189**, 539 (1991); A. Rouco, X. Obrador, M. Tovar, F. Pérez, D. Chateigner, and P. Bordet, Phys. Rev. B **50**, 9924 (1994).

[6] P. Adelmann, R. Ahrens, G. Czjzek, G. Roth, H. Schmidt, and C.Steinleitner, Phys. Rev. B **46**, 3619 (1992).

[7] M. Tovar, X. Obradors, F. Pérez, S. Oseroff, R.J. Duro, J. Rivas, D. Chateigner, P. Bordet, and J. Chenevas, Phys. Rev. B **45**, 4729 (1992).

[8] A.A. Stepanov, P. Wyder, T. Chattopadhyay, P.J. Brown, G. Fillion, I.M. Vitebsky, A. Deville, B. Gaillard, S.N. Barilo, and D.I. Zhigunov, Phys. Rev. B **48**, 12 979 (1993).

[9] E.T. Heyen, R. Liu, M. Cardona, S. Piñol, R.J. Melville, D. McK. Paul, E. Morán, and M.A. Alario-Franco, Phys. Rev. B **43**, 2857 (1991).

[10] M.A. Laguna, M.L. Sanjuán, A. Butera, M. Tovar, Z. Fisk, and P. Canfield, Phys. Rev. B **48**, 7565 (1993).

[11] M. Udagawa, Y. Nagaoka, N. Ogita, M. Masada, J. Akimitsu, and K. Ohbayashi, Phys. Rev. B **49**, 585 (1994).

[12] K.A. Kubat-Martin, Z. Fisk, and R. Ryan, Acta Crystallogr. C **44**, 1518 (1988).

[13] D.B. Wiles and R.A. Young, J. Appl. Crystallogr. **14**, 149 (1981).

[14] E.T. Heyen, G. Kliche, W. Kress, W. König, M. Cardona, E. Rampf, J. Prade, U. Schröder, A.D. Kulkarni, F.W. de Wette, S. Piñol, D. McK. Paul, E. Morán, and M.A. Alario-Franco, Solid State Commun. **74**, 1299 (1990).

[15] E. Rampf, U. Schröder, F.W. Wette, D. Kulkarni, and W. Kress, Phys. Rev. B **48**, 10 143 (1993).

[16] S. Jandl, M. Iliev, C. Thomsen, T. Ruf, M. Cardona, B.M. Wanklyn, and C. Chen, Solid State Commun. **87**, 609 (1993).

[17] J.A. Sanjurjo, C. Rettori, S. Oseroff, and Z. Fisk, Phys. Rev. B **49**, 4391 (1994).

[18] Ph. Galez, P. Scheiweiss, G. Collin, and R. Bellinset, J. Less-Common Met. **164-165**, 784 (1990).

[19] C. Rettori, S.B. Oseroff, D. Rao, J.A. Valdivia, G.E. Barberis, G.B. Martins, J. Sarrao, Z. Fisk, and M. Tovar (unpublished).

[20] R.D. Zysler, A. Butera, A. Fainstein, M. Tovar, and Z. Fisk, J. Appl. Phys. **73**, 5680 (1993).

[21] N. Suzuki and H. Kamimura, J. Phys. Soc. Jpn. **35**, 985 (1973).

[22] D. Fuchs, M. Noll, A. Grauel, C. Geibel, and F. Steglich, Physica B **194-196**, 2255 (1994).

[23] G.H. Huang, J.H. Shieh, and H.C. Ku, Physica C **185-189**, 1163 (1991).

[24] C. Lin, G. Lu, Z. Liu, and Y. Shang, Solid State Commun. **84**, 721 (1992).

[25] C. Lin, G. Lu, Z. Liu, and Y. Shang, Physica C **194**, 66 (1992).

[26] Y. Nagata, T. Okamoto, N. Suzuki, T. Uchida, M.D. Lan, L. Zhang, P. Klavins, and R.N. Shelton, Physica C **185-189**, 1109 (1991).

[27] T. Schultz, R. Smith, A. Fondado, C. Maley, T. Beacon, P. Tinklenberg, J. Gross, C. Saylor, S. Oseroff, Z. Fisk, S.-W. Cheong, and T.E. Jones, J. Appl. Phys. **75**, 6723 (1994).